NeuroImage: Clinical 32 (2021) 102876

Contents lists available at ScienceDirect

NeuroImage: Clinical

journal homepage: www.elsevier.com/locate/ynicl

Neurophysiological characteristics in the periventricular/periaqueductal gray correlate with pain perception, sensation, and affect in neuropathic pain patients

Huichun Luo [a,b,1], Yongzhi Huang [c,1], Alexander L. Green [d], Tipu Z. Aziz [d], Xiao Xiao [b,e], Shouyan Wang [b,e,f,*]

[a] Shanghai Key Laboratory of Psychotic Disorders, Shanghai Mental Health Center, Shanghai Jiao Tong University School of Medicine, Shanghai, China
[b] Institute of Science and Technology for Brain-Inspired Intelligence, Fudan University, Shanghai, China
[c] Academy of Medical Engineering and Translational Medicine, Tianjin University, Tianjin, China
[d] Nuffield Department of Surgical Sciences and University of Oxford, John Radcliffe Hospital, Oxford, UK
[e] Key Laboratory of Computational Neuroscience and Brain-Inspired Intelligence (Fudan University), Ministry of Education, China
[f] Engineering Research Center of AI & Robotics, Ministry of Education, Fudan University, Shanghai, China

ARTICLE INFO

Keywords:
Periventricular/periaqueductal gray
Local field potential
Neural oscillation
Dynamic neural state
Local network
Pain components

ABSTRACT

The periventricular/periaqueductal gray (PAG/PVG) is critical for pain perception and is associated with the emotional feelings caused by pain. However, the electrophysiological characteristics of the PAG/PVG have been little investigated in humans with chronic pain. The present study analyzed the oscillatory characteristics of local field potentials (LFPs) in the PAG/PVG of eighteen neuropathic pain patients. Power spectrum analysis and neural state analysis were applied to the PAG/PVG LFPs. Neural state analysis is based on a dynamic neural state identification approach and discriminates the LFPs into different neural states, including a single neural state based on one oscillation and a combinational neural state based on two paired oscillations. The durations and occurrence rates were used to quantify the dynamic features of the neural state. The results show that the combined neural state forms three local networks based on neural oscillations that are responsible for the perceptive, sensory, and affective components of pain. The first network is formed by the interaction of the delta oscillation with other oscillations and is responsible for the coding of pain perception. The second network is responsible for the coding of sensory pain information, uses high gamma as the main node, and is widely connected with other neural oscillations. The third network is responsible for the coding of affective pain information, and beta oscillations play an important role in it. This study suggested that the combination of two neural oscillations in the PAG/PVG is essential for encoding perceptive, sensory, and affective measures of pain.

1. Introduction

Chronic pain is a complex multidimensional experience encompassing sensory, affective, and cognitive components, all of which interact and contribute to the final response of an individual who is subjected to pain (Auvray, et al., 2010). These multidimensional components of pain experiences are encoded by distributed brain networks. Numerous human neuroimaging studies have suggested that a large set of brain regions, such as the primary sensory cortex (S1), anterior cingulate cortex, orbitofrontal cortex, anterolateral prefrontal areas, insula, thalamus, amygdala, and brainstem, play important roles in pain processing and modulation (Borsook, et al., 2010; Davis, et al., 2017).

The periaqueductal gray (PAG) is an anatomic and functional interface between the forebrain and the lower brainstem. It has been implicated in multiple cognitive and physiological processes, including pain perception and sensory and emotion information coding

Abbreviations: PAG/PVG, periventricular/periaqueductal gray; LFP, local field potential; DBS, deep brain stimulation; VAS, visual analog scale; MPQ, the McGill pain questionnaire.

* Corresponding author at: Institute of Science and Technology for Brain-Inspired Intelligence, Fudan University, Shanghai, 220 Handan Road, Yangpu District, Shanghai, 200433, PR China.
E-mail address: shouyan@fudan.edu.cn (S. Wang).

[1] These authors contribute equally to this work

https://doi.org/10.1016/j.nicl.2021.102876
Received 15 July 2021; Received in revised form 9 October 2021; Accepted 3 November 2021
Available online 10 November 2021

(Behbehani, 1995; Green and Paterson, 2020; Krout and Loewy, 2000). It has been found that stimulation of the PAG produces the sensation of burning pain and fear (Nashold, et al., 1969), and lesions of the ventrolateral area of the PAG in cats significantly attenuated the perception of pain (Melzack, et al., 1958). Moreover, the PAG receives afferents from nociceptive neurons in the spinal cord and has also been found to be associated with pain transmission (Keay, et al., 1997). More direct evidence of the involvement of the PAG in pain processing in humans comes from the fact that stimulation of the PAG has therapeutic effects for treating neuropathic pain (Boccard, et al., 2013; Gray, et al., 2014). These findings seem contradictory to some extent, i.e. the PAG could be involved in pain sensitization/induction as its inhibition/lesion reduces pain, and it yet also inhibits pain by endogenous pain inhibition. There might be microcircuitries within the PAG, which lead to complex coding and modulating of the pain processing. Therefore, the role of the PAG in different components in chronic pain, including pain perception, sensory, and affective pain, still needs more elaboration.

The neural decoding of different pain components in the PAG could be critical for revealing pain processing mechanisms in the brain (Neumann, et al., 2019; Shirvalkar, et al., 2018). This might also shed light on how to modulate the PAG in the treatment of chronic pain. It has been suggested that pain information can be coded with a single neural oscillation and with the integration of multiple neural oscillations with different frequencies in the brain (Ploner, et al., 2017). In addition, it has become apparent that brain states dynamically fluctuate among different perceptual, cognitive, and emotional processes. Our previous study in humans showed that in deep brain areas (such as the sensory thalamus), different neural oscillations are integrated, resulting in two distinct oscillatory networks responsible for pain perception and pain modulation by a dynamic neural state identification approach (Luo, et al., 2018; 2019). In this study, we utilized the unique opportunity offered by deep brain stimulation (DBS) surgery targeting the PAG/PVG as a clinical treatment for neuropathic pain. The resting local field potentials (LFPs) were measured from the PAG area using electrodes implanted for DBS in patients. This study aimed to decode the neural representations of the perceptive, sensory, and affective characteristics of neuropathic pain in PAG/PVG neural activity. The dynamic neural state in the PAG/PVG was characterized by previously developed dynamic neural state analysis (Luo, et al., 2018). The correlations between measures of neural states and three pain dimensions (perception, sensation, and affect) were investigated. Finally, a linear regression model was used to predict pain scores from the three dimensions based on the neural state of LFPs. The results aim to disentangle the involvement of PAG/PVG oscillatory networks in coding different dimensions of neuropathic pain.

2. Material and methods

2.1. Participants

Eighteen neuropathic pain patients (age: 47.9 ± 10.4 years, mean ± SD) were recruited for this study. All patients underwent DBS surgery at the John Radcliffe Hospital, Oxford, UK. The detailed procedures of DBS surgery, including targeting and DBS electrode (quadripolar macroelectrode, Model 3387, Medtronic, Minneapolis, MN, USA) implantation, have been reported in previous work (Green, et al., 2009; Pereira, et al., 2013; Wu, et al., 2014). After surgery, the localization of DBS electrodes was confirmed by postoperative MRI. An example of the reconstructed location of the DBS electrode of a patient is shown in Fig. 1A. All patients signed an informed written consent form, and this study was carried out in accordance with the Declaration of Helsinki and received approval from the Oxford Research Ethics Committee B (project number: 13SC0298).

2.2. Clinical measures

Quantitative assessments of pain and health-related quality of life were performed before DBS surgery. Both the visual analog scale (VAS, 0–10) (Huskisson, 1974) and the McGill pain questionnaire (MPQ) (Melzack, 1975) were used. The VAS had anchors of “no pain” (0) and “the worst pain you can imagine” (10). Since the pain intensity strongly fluctuated, the patients recorded the VAS rating twice daily in a pain diary for 7 days. There were 14 VAS scores reviewed for each patient to ensure appropriately completed records, and the mean value was then calculated and considered the preoperative pain perception. The MPQ provided additional quantitative information in the domains of “sensory,” “affective”, “evaluative”, and “miscellaneous” pain severity. There were ten questions to assess the sensory domain for sensory pain,

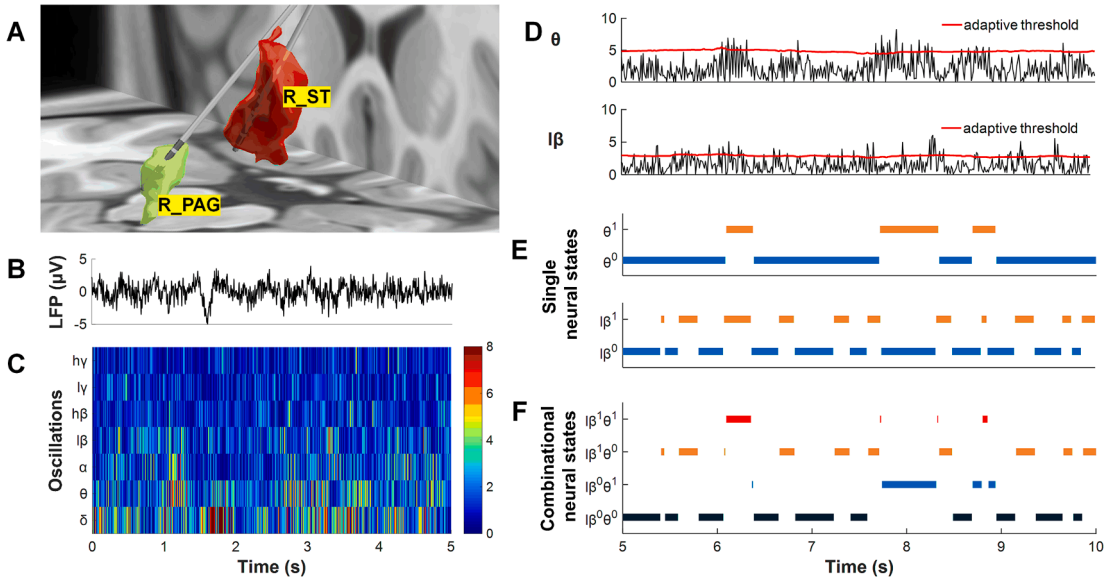

Fig. 1. LFPs recorded from the PAG/PVG and a brief procedure for neural state calculation. The electrodes of patient No. 3 were visualized in 3-D using the lead-DBS toolbox (A). Single neural states and combinational neural states were identified by the dynamic neural state identification (DNSI) approach (B-F). R_PAG: right PAG, R_ST: right sensory thalamus. The superscript numbers indicate the activity state of neural oscillations; “0″ represents the desynchronization state, while “1” represents the synchronization state.

including pain location, duration, and properties, and five questions to assess the affective domain of pain.

Three dimensions of pain-related scores were used in this study: pain perception was assessed by the VAS score, and pain sensation and pain affective dimension were assessed by the total score of the sensor part and the total score of the affective part in the MPQ questionnaire, respectively.

2.3. Local field potential recording and preprocessing

PAG/PVG local field potentials (LFPs) were recorded through electrode extension cables 3–5 days after electrode implantation. The experiment was carried out after at least 12 h medication off. Moreover, the experiment was carried out after 12 h of DBS was turned off if patients had brief DBS for clinical test. PAG/PVG LFP recordings were performed at rest from adjacent pairs (01, 12, 23) with a common electrode placed on the surface of the mastoid. The LFPs were amplified (×10,000; CED 1902 amplifier, Cambridge Electronic Design, Cambridge, UK), filtered with a 0.5–500 Hz bandpass filter, and recorded at a sampling rate of 2000 Hz (CED 1401 Mark II, Cambridge Electronic Design, UK). From each electrode, only the LFPs recorded from the contacts used for postoperative chronic stimulation were selected. Patient No. 14 underwent bilateral PAG/PVG implantation, but only the left side of the PAG/PVG LFP was chosen since the pain intensity was more severe on the right side. Hence, LFP recordings from 18 PAGs were chosen for analysis.

The selected LFPs were preprocessed with a low-pass filter at 90 Hz, an adaptive notch filter to remove 50 Hz line noise, and a high-pass filter at 2 Hz to eliminate baseline shifting. Finally, all signals were downsampled to 500 Hz. A continuous 50-second sample was selected from total 3–5 min recordings for further analysis. These 50-second segments were free of artifacts.

2.4. Dynamic neural state analysis

It has been proven that the high level of oscillations in LFPs is the product of synchronized subthreshold activity across large populations of local neuronal elements (Hammond, et al., 2007). Therefore, real-time detection of changes in the activity level of neural oscillations can reflect the dynamic activities of the synchronization and desynchronization of the neuron population (Buzsaki and Draguhn, 2004; Sakurai, 1999). The dynamic neural state identification (DNSI) approach we previously established is a method that can reliably detect the dynamic level of neural oscillation activity (Luo, et al., 2018). The DNSI divides the activity level of neural oscillation into a synchronization state and a desynchronization state, which correspond to neural oscillation states of high activity levels and low activity levels, respectively.

As shown in Fig. 1B–C, through wavelet packet (WP) transform, the activity of neural oscillation is characterized by wavelet packet coefficients (WPCs). The WPC not only reflects the activity level of neural oscillations but can also differentiate regular patterns in oscillations from random patterns (Donoho and Johnstone, 1994). Then, an adaptive threshold is used to discriminate neural oscillations into synchronization and desynchronization states and annotated as 1 or 0, respectively (Fig. 1D). Finally, if only one neural oscillation is selected to define the neural state of the LFPs, such as theta oscillation, there are two single neural states: θ^1 and θ^0 (Fig. 1E). If two neural oscillations are selected to define the neural states, such as theta and low-beta oscillations, there are four combinational neural states: $l\beta^0\theta^0$, $l\beta^0\theta^1$, $l\beta^1\theta^0$, and $l\beta^1\theta^1$ (Fig. 1F). The advantage of using the DNSI approach is that it uses the WP transform to improve the signal-to-noise ratio of the oscillations while highlighting patterned neural activity, and it uses adaptive thresholds to better capture the dynamic changes in neural activity (Luo, et al., 2018).

To quantify the dynamic characteristics of the neural state, two measures, the duration and occurrence rate, are calculated. The duration is the average duration of occurrences of one neural state:

$$\text{Duration} = \frac{\sum_{i=1}^{N} t_i}{N} \quad (1)$$

where t_i is the duration of the i^{th} occurrence of one neural state and N is its total number of occurrences within a certain time.

The occurrence rate of one neural state is the number of occurrences within one minute:

$$\text{Occurrence rate} = \frac{N}{T_{total}} \cdot 60 \quad (2)$$

where T_{total} is the total time of the LFPs.

2.5. Data analysis and statistics

First, the power spectra of LFPs were calculated using the windowed fast Fourier transform with a 2-second sliding window with 1-second of overlap. To reduce the influence of between-subject variability, the power spectra were normalized by using a z-transformation within 2–90 Hz.

Second, the neural state of the PAG/PVG LFPs was defined by one oscillation or two oscillations by applying the DNSI approach. According to common neural oscillation frequency bands and pain electrophysiological research, the PAG/PVG LFPs were divided into seven frequency band oscillations for neural state analysis: delta (δ, 3–6 Hz), theta (θ, 6–9 Hz), alpha (α, 9–12 Hz), low-beta (lβ, 12–24 Hz), high-beta (hβ, 24–36 Hz), low-gamma (lγ, 36–60 Hz) and high-gamma (hγ, 60–90 Hz). Compared to our previous study (Luo, et al., 2019), the activity state of oscillation was slightly modified since a very short synchronization state may be induced by noise or identification error (Tinkhauser, et al., 2017a; b). In this study, a synchronization state shorter than 2 periods of the center frequency of oscillation was corrected to the desynchronization state. Combinational neural states were defined based on each pair of the seven oscillations. Then, dynamic measures of the duration and occurrence rate of single or combinational neural states were calculated.

Correlations between normalized power spectra and the VAS, sensory and affective scores were evaluated with the Pearson correlation test. The normalized power spectra were calculated every 0.5 Hz over 2–90 Hz. The significance of a correlation was assessed with a conservative criterion that requires that three or more consecutive bins reach $p < 0.01$. Then, correlations between the duration and occurrence rate measures of the neural states and the perceptive, sensory, and affective pain scores were also evaluated by the Pearson correlation test. To compensate for the multiple comparisons between the measures of multiple neural states and pain scores, a false discovery rate (FDR) correction (Benjamini and Hochberg, 1995) was performed. All null hypotheses were rejected by a two-tailed alpha threshold of p value less than 0.05 (corrected with FDR).

To predict pain scores, features that were significantly correlated with perceptive, sensory, and affective scores were integrated by principal component analysis (PCA). Then, a linear model was developed based on the critical components of the features, and the predicted value was limited by the range of pain scores. For example, the smallest prediction value was 0, and the highest was 10, since the range of the VAS score is from 0 to 10. The prediction models were further validated using a leave-one-out cross-validation approach. According to the leave-one-out approach, the data from each patient were selected as the test dataset, and the data from the other seventeen patients were used as the training dataset to build the model. The predictive performance of the model was evaluated in terms of prediction error between the predicted and actual pain scores as follows:

$$Prediction error = \frac{|\text{true\_value-predicted\_value}|}{\text{Max-Min}} \cdot 100\% \quad (3)$$

The prediction error was the percentage of the difference between

the true value and predicted value relative to the range of scores. The number of principal components used to build a linear model for pain score prediction was directly determined by the prediction error. First, all principal components were ranked by the variance in the pain score that they had accounted for. Second, we chose the first n principal components to build a prediction model (where 1<= n <= N and N is the total number of significant features). Finally, n was optimized by comparing the prediction error of the models. The optimal prediction model can be expressed as follows:

$$V\_predict = a - \sum_{i=1}^{n} b_i \cdot x_i \quad (4)$$

The predicted value was obtained from a linear model based on the first n principal components, where 'a' and 'b_i' are the coefficients of the linear regression model.

In this study, signal analysis was conducted using MATLAB (Version 9.1, MathWorks, Inc., Natick, MA, USA), and statistical analyses were conducted using MATLAB and SPSS (Version 22, IBM, New York, NY, USA).

3. Results

Table 1 presents the demographic and clinical characteristics of each of the 18 patients (16 males and 2 females; age: 47.9 ± 10.4 years) enrolled in this study. Six patients were diagnosed with stroke pain, four were diagnosed with phantom limb pain, and the remaining eight patients had other types of neuropathic pain. The pain perception assessed by the VAS score ranged from 4.8 to 10 (7.5 ± 1.6, mean ± SD). The total MPQ score ranged from 14 to 59 (35.1 ± 12.5, mean ± SD), with the sensory subitem ranging from 7 to 33 (19.7 ± 7.3, mean ± SD) and the emotion subitem ranging from 0 to 9 (4.9 ± 2.7, mean ± SD). The relationships among these three scores are illustrated in Table 2. There was no significant correlation between the VAS scores and the sensory score, the affective score, or the sum of the sensory and affective scores.

3.1. Correlations of neural states and pain components

Two measures of a single neural state and their correlation with pain scores are shown in Fig. 2A–B. The duration of the neural state shortened as the frequency of the neural state increased. Unexpectedly, the duration of $l\gamma^1$ was slightly higher than those of the surrounding $h\beta^1$ and $h\gamma^1$. However, no durations of the neural states were significantly associated with the perceptive, sensory, or affective pain scores. The distribution of the occurrence rates of the neural state was the opposite of the duration measure; the higher the frequency of the neural state was, the higher the occurrence rate. In addition, neural state $h\gamma^1$ showed an abnormal increase. No significant relationship was found between the occurrence rates and pain scores.

A combinational neural state was defined by the paired activity states of two oscillations. We analyzed not only the correlations between durations and pain scores but also the correlations between occurrence rates and pain scores. The results are shown in Fig. 3A–B. Similar to the single neural states, when one component of the combinational neural states was the same, the other component was a low-frequency oscillation with a longer duration than the high-frequency oscillation; for example, the duration of neural state $\theta^0\delta^0$ was higher than that of neural state $h\gamma^0\delta^0$. Moreover, a combinational neural state with a desynchronization component had a longer duration than one that did not; for example, the duration of $\theta^0\delta^0$ was longer than that of neural state $\theta^0\delta^1$. However, the occurrence rates had a different distribution than the other duration measures. When one component of the combinational neural states was the same, the other component was a high-frequency oscillation that had a higher occurrence rate than the low-frequency oscillation; for example, the occurrence rate for neural state $h\gamma^0\delta^0$ was higher than that for neural state $\theta^0\delta^0$. Combinational neural states with desynchronization components had higher occurrence rates than those without desynchronization components; for example, the occurrence rate of $\theta^0\delta^0$ was higher than that of the neural state $\theta^0\delta^1$.

We found broader and more marked correlations between measures

Table 1
Clinical information of subjects.

No.	Age/Sex	Etiologies	Targets	Pain distribution	Pre-op VAS	Pre-op MPQ			
						Sensory	Affective	Miscellaneous	Total
1	60/M	Stroke pain	L_PAG/PVG L_ST	Hemibody	9.2	31	8	9	53
2	39/M	Trigeminal neuralgia	R_PAG/PVG R_ST	Left supraorbital	7.5	33	9	12	59
3	40/F	Intractable forehead pain	R_PAG/PVG R_ST	Focal	5	13	5	2	23
4	38/M	Phamton limb pain	R_PAG/PVG R_ST	Left arm	8	7	2	3	17
5	43/M	Phamton limb pain	R_PAG/PVG R_ST	Left leg	5.6	22	5	5	35
6	53/M	Brachial plexus injury	L_PAG/PVG L_ST	Focal	4.8	22	6	7	39
7	54/M	Poststroke pain	R_PAG/PVG R_ST	Hemibody	6.7	18	2	6	29
8	58/M	Facial pain	L_PAG/PVG L_ST	Focal	9	22	7	9	43
9	35/M	Poststroke pain	L_PAG/PVG L_ST	Focal	9	16	5	6	32
10	42/M	Radiculo/plexopathy	L_PAG/PVG L_ST	Focal	10	29	0	5	35
11	58/M	Phamton limb pain	R_PAG/PVG	Phantom limb	7	22	5	14	46
12	34/M	Cephalalgia	R_PAG/PVG	Vertex	6.4	18	7	3	32
13	56/M	Amputation	R_PAG/PVG	Stump	7	13	5	6	24
14	46/F	Phamton limb pain	bilateral PAG/PVG	phantom limb	6.4	20	3	5	31
15	53/M	Stroke pain	R_PAG/PVG	Left arm	10	7	2	1	14
16	62/M	Stroke pain	L_PAG/PVG	Right arm	8.43	16	1	4	25
17	61/M	Stroke pain	L_PAG/PVG	Face	7.4	19	7	12	42
18	31/M	Radiculo/plexopathy	PAG/PVG	Focal	6.67	27	9	11	52

pre-op: pre-operation (DBS surgery); VAS: visual analog scale; MPQ: the McGill pain questionnaire. In the "Targets" column, L means left brain, R means right brain, ST is the sensory thalamus, PAG/PVG is the periventricular/periaqueductal gray.

Table 2
Correlation between VAS score and different part of MPQ.

Correlation	Sensory	Affective	Evaluate	Miscellaneous	Sensory + Affective	MPQ total
r-value	0.021	−0.253	0.134	−0.014	−0.06	−0.032
p-value	0.9321	0.296	0.584	0.954	0.8058	0.9

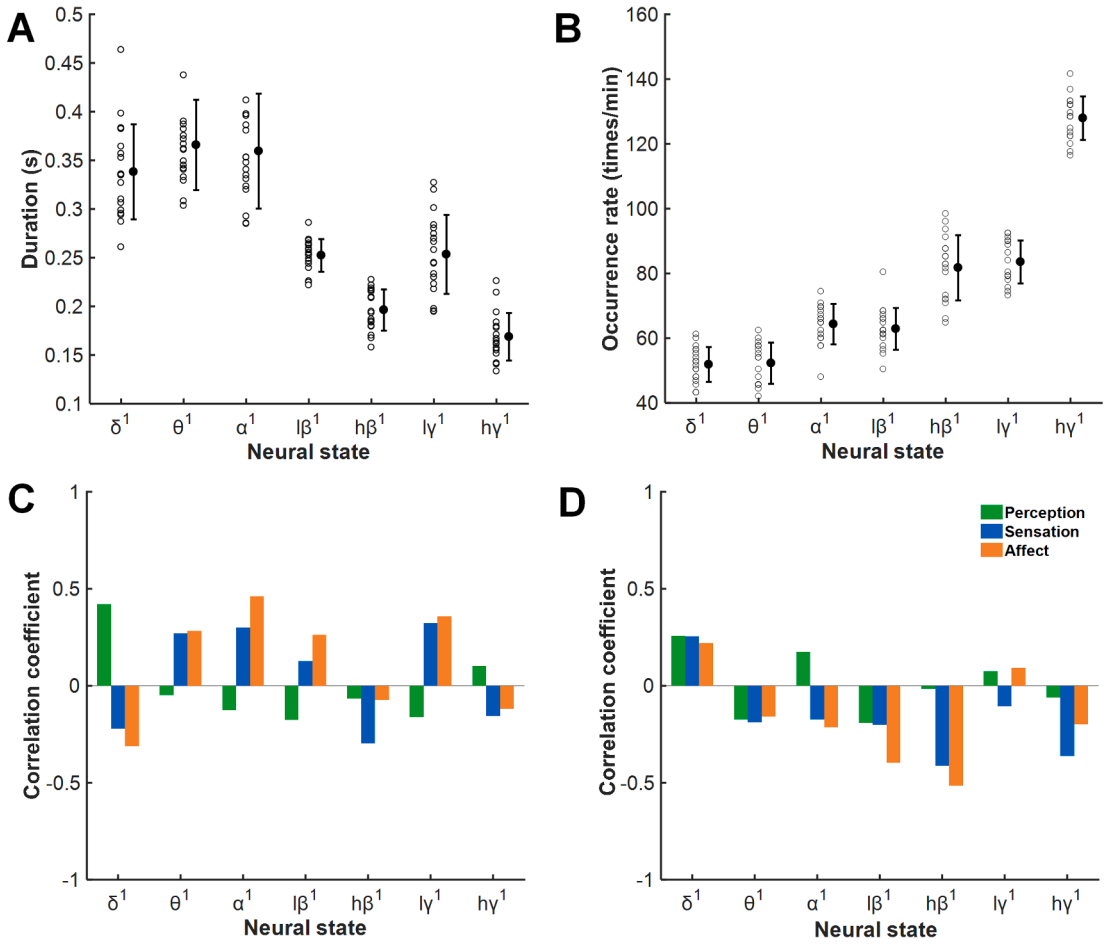

Fig. 2. Correlations between measures of single neural states and pain perception, sensation, and affect scores. The durations and occurrence rates of single neural states (A, B) and their correlations with pain perception, sensation, and affect scores (C, D). There were no significant correlations between neural state measures and pain measures.

of combinational neural states and pain scores than the measures of single neural states and pain scores (Fig. 3C–H). Regarding pain perception, the durations of two neural states, $l\beta^0\delta^1$ (r = 0.678, p = 0.008) and $l\gamma^0l\beta^1$ (r = -0.579, p = 0.047), and the occurrence rates of four neural states, $\theta^0\delta^1$ (r = 0.605, p = 0.031), $\alpha^0\delta^1$ (r = 0.636, p = 0.014), $\alpha^1\delta^1$ (r = 0.613, p = 0.014), and $l\gamma^0\delta^1$ (r = 0.722, p = 0.003), were significantly correlated, and most of these contained a synchronized state of delta oscillation. Regarding sensory pain, five duration measures, $h\gamma^0\delta^1$ (r = 0.687, p = 0.007), $h\gamma^0\theta^1$ (r = 0.762, p = 0.001), $h\gamma^0l\beta^0$ (r = 0.642, p = 0.016), $h\gamma^0l\gamma^0$ (r = 0.528, p = 0.048), and $h\gamma^1l\gamma^1$ (r = 0.537, p = 0.048), and two occurrence rate measures, $h\gamma^1\alpha^0$ (r = -0.600, p = 0.034) and $h\gamma^1l\beta^0$ (r = -0.628, p = 0.021), were significantly correlated, and most of them were based on the desynchronization state of high-gamma oscillation. Regarding affective pain, significant correlations were found in the duration of two neural states, $\alpha^1\theta^0$ (r = 0.626, p = 0.022) and $h\beta^0\alpha^1$ (r = 0.592, p = 0.039), and the occurrence rates of three neural states, $h\beta^1\theta^0$ (r = -0.590, p = 0.040), $l\gamma^0l\beta^1$ (r = -0.658, p = 0.012), and $l\gamma^0h\beta^0$ (r = -0.575, p = 0.050). The linear correlations between the most significant neural state and the pain perception, sensation, and affect scores are shown in Fig. 3I–K. All relationships between combinational neural states and pain scores are shown in Supplementary Fig. 1.

3.2. Pain score prediction based on multiple integrated LFP features

As shown in Fig. 3, almost all neural states that were significantly correlated with perception scores contained a delta oscillation component, with the exception of the duration of neural state $l\gamma^0l\beta^1$. Similarly, all neural states that were significantly related to the sensation scores contained a high-gamma oscillation component. However, no dominant components were found in these significant neurological states. As the results showed, there were a total of 6 significant features for the pain perception scores, including the duration of neural states $l\beta^0\delta^1$ and $l\gamma^0l\beta^1$ and the occurrence rate of neural states $\theta^0\delta^1$, $\alpha^0\delta^1$, $\alpha^1\delta^1$, and $l\gamma^0\delta^1$. There were total of 7 significant features for the sensation scores, including the duration of neural states $h\gamma^0\delta^1$, $h\gamma^0\theta^1$, $h\gamma^0l\beta^0$, $h\gamma^0l\gamma^0$, and $h\gamma^1l\gamma^1$ and the occurrence rate of neural states $h\gamma^1\alpha^0$ and $h\gamma^1l\beta^0$. There were total of 5 significant features for the affect scores, including the duration of neural states $\alpha^1\theta^0$ and $h\beta^0\alpha^1$ and the occurrence rates of neural states $h\beta^1\theta^0$, $l\gamma^0l\beta^1$, and $l\gamma^0h\beta^0$. The performance of the prediction models was based

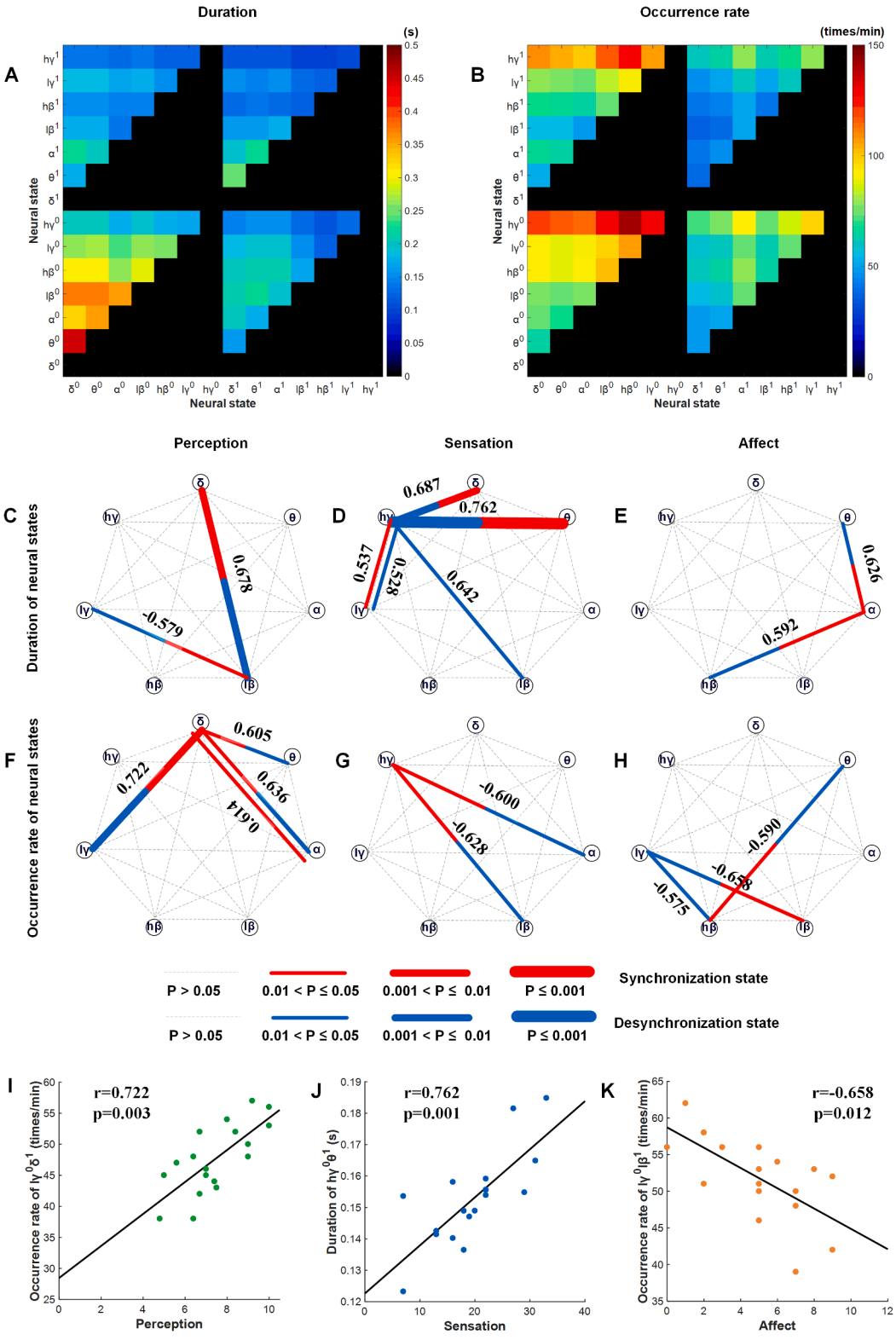

Fig. 3. Dynamic features of combinations of neural states and their relationship to clinical pain state measures. The duration (A) and occurrence rate (B) of the combinational neural states of each pair of combined oscillations. Correlations between the durations and occurrence rates of the combinational neural states for each pair of combined oscillations and pain perception, sensation and affect scores are shown in C–H. Significance is indicated by the width of the lines, and the numbers are the correlation coefficients. I-K are the linear correlations between the most significant neural state and the pain perception, sensation, and affect scores, respectively.

on different numbers of principal components. The lowest prediction error was obtained when only the first principal component was used for perception scores, the first two for sensory pain scores, and the first three for affective pain scores. The coefficient of each significant feature in the selected principal components is listed in Supplementary Tables 1–3. As shown in Fig. 4, for the perception score prediction, the correlation between the predicted value and the true perceptive score was higher than that for any feature ($r = 0.858$, $p = 0.000005$), and the prediction error was 7.18% ± 3.42%. For the sensation score prediction, the correlation between the predicted value and the real sensory pain score was higher than that for any LFP feature ($r = 0.805$, $p = 0.00006$), and the prediction error was 8.35% ± 5.85%. For the affect score prediction, compared to LFP features, the correlation between the predicted value and the real affect score was still higher ($r = 0.772$, $p = 0.0002$), and its

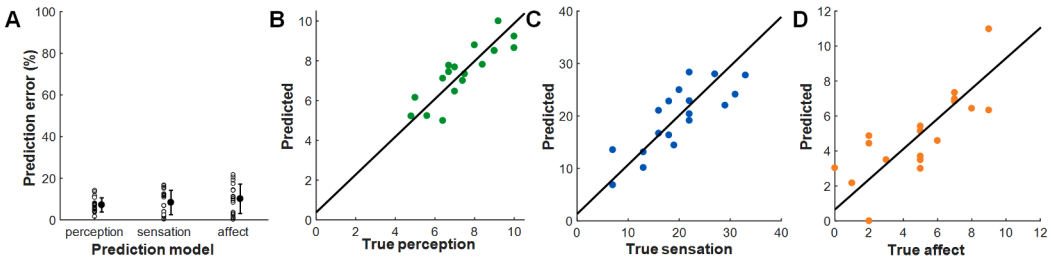

Fig. 4. The best prediction model power for the three pain components. Prediction errors of the best model for predicting pain perception, sensation, and affect scores (A). B-D are the linear correlations between the predicted value from the best prediction model and the true pain perception, sensation, and affect, respectively.

prediction error was 10.12% ± 7.05%.

4. Discussion

The present study reported the multidimensional pain coding neural features in the PAG/PVG. The dynamic features of different oscillatory bands correlated to perceptive, sensory, and affective dimensions of chronic pain. This result agreed with the fact that the PAG/PVG consists of both descending and ascending pathways in pain processing. It is involved in multiple functions related to pain as an essential nucleus. Modulating different oscillatory activities in the PAG/PVG may treat specific dimensions of the experience of pain in chronic pain patients.

4.1. Implication and application of pain perception, sensory pain and affective pain

Pain is a multidimensional complex experience with three dimensions: sensory-discriminative, affective-motivational and cognitive-evaluative dimensions (Melzack, 1975; Katz and Melzack, 1999). In this study, we correlated neural oscillations with sensory-discriminative pain and affective-motivational pain by using the VAS pain score and MPQ questionnaire with chronic pain patients. Due to the complexity of the cognitive-evaluative dimension and the simplification of the evaluative domain in the MPQ questionnaire, we will discuss it in future studies. Here, the sensory domain and the affective domain of the MPQ questionnaire were used to measure sensory pain and affective pain, respectively. The pain sensory information includes the dynamic characteristics, including the sensory pain score, associated with information on the duration, location, time, and properties of pain, which was specifically encoded by an oscillation network centered at high-gamma oscillation (Fig. 5). The emotion-affective dimension of pain includes immediate pain unpleasantness and a motivational component that is also called the "secondary pain affect" (Price, 2000, 2002). Consistent with this, we found that several neural oscillations are involved in the encoding of affective pain information (Fig. 5), and this may be due to the complexity of emotional circuits.

As a unidimensional instrument, the VAS pain score specifically and primarily reflects the intensity of pain perceptual experience, which is correlated with pain perception here. In this study, pain perception is highly correlated with delta oscillation (Fig. 5). However, somatosensory localization and intensity coding are sometimes linked with moment-by-moment (autonomic) pain unpleasantness (Fields, 1999). Interestingly, neural states based on delta combined with other oscillations have more marked relationships with pain perception scores than single delta neural states, indicating that perception as an overall reflection of the pain state may contain complex information and involve additional brain areas. With reproducible results, the VAS is easy to measure, is sensitive to treatment effects, and is most widely used to evaluate pain severity and relief (Todd, 1996). The extent of the measured outcomes in VAS and the neural features correlated with pain perception we identified here might be potential biomarkers for future clinical applications.

4.2. Neural oscillations in the PAG and its biological features

The PAG/PVG receives afferents from nociceptive neurons in the spinal cord and sends ascending projections to many parts of the thalamus, which indicates that the abnormal oscillatory network in the PAG/PVG may be related to pathological changes in other brain areas, especially thalamocortical dysrhythmia, which has been proven to be an important mechanism involved in chronic pain (An et al., 1998; Berendse and Groenewegen, 1990, 1991; Devinsky et al., 1995; Hartley

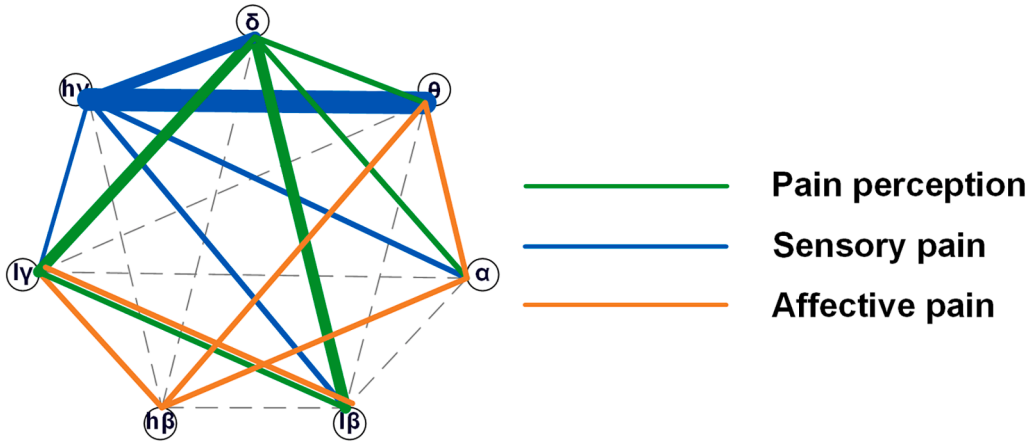

Fig. 5. A summary of correlations between neural state measures and pain perception, sensory pain, and affective pain. The colored lines between two oscillations indicate significant correlations between neural states based on these two combined oscillations and pain. Different colors represent different dimensions of pain, as listed in the legend, and the line width represents the importance of this combinational neural state for pain components.

et al., 2017; Krout and Loewy, 2000). In this study, we found the importance of delta oscillations for pain perception (Fig. 5), which is highly consistent with our previous results that a neural network centered on delta oscillations in the sensory thalamus is responsible for neuropathic pain perception (Luo, et al., 2019). Many studies have reported that oscillations below 10 Hz are changes in the thalamus and S1, as well as the coupling between the thalamus and S1, in laser-induced pain, inflammatory pain, and neuropathic pain (Li, et al., 2017; Sarnthein and Jeanmonod, 2008; Sarnthein, et al., 2003; Stern, et al., 2006; Wang, et al., 2016).

The results also revealed that high-frequency gamma band oscillation may be a suitable biomarker to encode pain sensation. Oscillations in the gamma frequency band were induced by phasic pain stimuli over the sensorimotor cortex at latencies between 150 and 350 ms (Hauck, et al., 2007). Furthermore, gamma oscillations over brain areas shift from encoding sensory processes to encoding emotional-motivational phenomena after a few minutes of stimulation (Ploner, et al., 2017). On the other hand, the amplitude of gamma oscillations in S1 could predict the pain intensity induced by laser stimulation in both humans and rodents (Hu and Iannetti, 2019; Yue, et al., 2020) and the pain level in chronic pain patients (Parker, et al., 2020; Zhou, et al., 2018). Increased gamma activity was identified in the PAG after noxious laser stimulation in rats (Li, et al., 2017). Another human study reported elevated gamma oscillations in the dorsal PAG after naloxone infusions that indicated the sensation of more severe pain (Pereira, et al., 2013). These clues suggested that gamma oscillations may contain more specific information about pain, while low-frequency band oscillation may be a pathological sign of chronic pain.

This study found that a beta oscillation-centered network was significantly related to the pain emotional score, which may indicate that beta oscillations play a key role in encoding pain affect. Beta oscillations may arise from brain areas related to pain emotion because beta oscillations are believed to serve as a feedback signal (Michalareas, et al., 2016). A laser-induced pain study examining anterior cingulate cortex (ACC) activity in rats reported that delta and gamma oscillations increased, while beta oscillations decreased after laser stimulation (Li, et al., 2017). Another study in fibromyalgia patients found increased theta and beta oscillations in the middle frontal lobe and midcingulate gyrus, but individual differences in depression, anxiety, or negative affect did not account for these findings (Gonzalez-Roldan, et al., 2016).

4.3. PAG and its roles in the pain matrix

Activation of the PAG has been found to be a part of a descending pathway for attentional control of pain by using fMRI (Tracey, et al., 2002). Neuroanatomical studies have also suggested the PAG-mediated central modulation of ascending responses to pain. Nociceptive neurons located in laminae VII and VIII of the spinal cord and laminae V and VI of the SpV project to the PAG (Mouton and Holstege, 2000; Vanderhorst, et al., 1996), posterior hypothalamic nucleus (Çavdar et al., 2001), and intralaminar thalamic nuclei (Carstens and Trevino, 1978; Royce et al., 1991; Shigenaga, et al., 1983). The PAG-involved pain matrix has also been reported in all pain types, such as neuropathic pain (Samineni, et al., 2017), inflammatory pain (Li and Sheets, 2018), and cancer-induced bone pain (Xu, et al., 2021). In a recent study, dopamine neurons in the ventrolateral periaqueductal gray/dorsal raphe (vlPAG/DR) through projections to the bed nucleus of the stria terminalis (BNST) contributed to sex differences in regulating pain-related behaviors (Yu, et al., 2021).

The PAG/PVG involves at least three pathways related to affective aspects of pain. First, the ventrolateral, lateral, and rostral PAG directly project to the intralaminar and midline thalamic nuclei, which is the key node of the affective pain system (Xiao and Zhang, 2018). The PAG-thalamic-forebrain circuit is associated with emotional responses (Krout and Loewy, 2000). Second, there is a strong projection from the amygdala to the PAG. The amygdala is a part of the limbic system and has been proven to be related to emotional and affective components and memory inherent to painful experiences. Third, the PAG indirectly connects with the ACC through the right paracentral nucleus and the central medial nucleus and is therefore involved in the affective pain response since the dorsal ACC has been implicated in the affective aspects of pain (Boccard, et al., 2017; Osaka, et al., 2004; Russo and Sheth, 2015). Therefore, the neural coding mechanism of pain emotion needs more in-depth research.

In addition, we employed prediction models for three-dimensional information of neuropathic pain based on integration features from single signal LFPs of the PAG/PVG and obtained low prediction errors. Compared to other models based on complex algorithms (Wager, et al., 2013; Zhang, et al., 2013), this model has good interpretability based on a clear neural mechanism. There might be similar neural states and relevant local networks of oscillations in neurological diseases, such as Parkinson's disease, depression, and addiction. This work may provide a potential for developing a neural-state-dependent neuromodulation strategy for pain (Neumann, et al., 2019; Shirvalkar, et al., 2018) in the future.

5. Limitations

This study is subject to several limitations. First, we included only 18 subjects, and only two of them were female patients. Although we currently provide the largest known human dataset of LFPs recorded from the deep nucleus, a larger sample of research should be carried out, and more female subjects should be included in the future. Second, the etiologies of the recruited neuropathic pain patients are different. This is also a common problem in current chronic pain research, and perhaps more stable results could be obtained by using only one type of neuropathic pain in the future. Third, we did not carry out long-term LFP recordings and could not observe the relationship between the dynamics of neural activity and the dynamic changes in pain, which will be a very interesting question to explore.

6. Conclusion

In summary, this study reported that the PAG/PVG was involved in coding perception, sensory, and affective aspects of pain information, potentially through the integration of multiple oscillations within local networks. Distinct oscillatory networks in the PAG/PVG based on different key oscillations may help to elucidate the neural mechanisms of pain.

CRediT authorship contribution statement

Huichun Luo: Formal analysis, Methodology, Software, Writing – original draft, Writing – review & editing. **Yongzhi Huang:** Methodology, Writing – original draft, Writing – review & editing. **Alexander L. Green:** Investigation, Writing – original draft. **Tipu Z. Aziz:** Methodology, Writing – original draft. **Xiao Xiao:** Visualization, Writing – review & editing. **Shouyan Wang:** Formal analysis, Project administration, Funding acquisition, Writing – original draft, Writing – review & editing.

Declaration of Competing Interest

The authors declare that they have no known competing financial interests or personal relationships that could have appeared to influence the work reported in this paper.

Acknowledgments

We thank Professor Tifei Yuan for his critical reading and linguistic edit of the manuscript.

Funding source

This work is supported by the National Key R&D Program of China (No. 2018YFC1705800); Shanghai Municipal Science and Technology Major Project (No. 2021SHZDZX0103); Shanghai Municipal Science and Technology Major Project (No. 2017SHZDZX01); The Chinese Ministry of Education 111 Project (No. B18015); Shanghai municipal commission of science and technology Major Project (No. 2018SHZDZX01) and ZJLab, and Shanghai Center for Brain Science and Brain-Inspired Technology, the National Key R&D Program of China (No. 2019YFA0709504), the National Natural Science Foundation of China (NO. 31900719), Science and Technology Committee Rising-Star Program (No. 19QA1401400), Shanghai Sailing Program (No. 21YF1439700).

Appendix A. Supplementary data

Supplementary data to this article can be found online at https://doi.org/10.1016/j.nicl.2021.102876.

References

An, X., Bandler, R., Ongur, D., Price, J.L., 1998. Prefrontal cortical projections to longitudinal columns in the midbrain periaqueductal gray in macaque monkeys. J. Comp. Neurol. 401, 455–479.

Auvray, M., Myin, E., Spence, C., 2010. The sensory-discriminative and affective-motivational aspects of pain. Neurosci. Biobehav. Rev. 34, 214–223. https://doi.org/10.1016/j.neubiorev.2008.07.008/.

Behbehani, M.M., 1995. Functional-characteristics of the midbrain periaqueductal gray. Prog. Neurobiol. 46 (6), 575–605. https://doi.org/10.1016/0301-0082(95)00009-K.

Benjamini, Y., Hochberg, Y., 1995. Controlling the false discovery rate – a practical and powerful approach to multiple testing. J. R. Stat. Soc. Ser. B-Stat. Methodol. 57, 289–300. https://doi.org/10.1016/0301-0082(95)00009-k/.

Berendse, H.W., Groenewegen, H.J., 1990. Organization of the thalamostriatal projections in the rat, with special emphasis on the ventral striatum. J. Comp. Neurol. 299, 187–228. https://doi.org/10.1002/cne.902990206/.

Berendse, H.W., Groenewegen, H.J., 1991. Restricted cortical termination fields of the midline and intralaminar thalamic nuclei in the rat. Neuroscience 42, 73–102. https://doi.org/10.1016/0306-4522(91)90151-d/.

Boccard, S.G., Prangnell, S.J., Pycroft, L., Cheeran, B., Moir, L., Pereira, E.A., Fitzgerald, J.J., Green, A.L., Aziz, T.Z., 2017. Long-term results of deep brain stimulation of the anterior cingulate cortex for neuropathic pain. World Neurosurg. https://doi.org/10.1016/j.wneu.2017.06.173/.

Boccard, S.G.J., Pereira, E.A.C., Moir, L., Aziz, T.Z., Green, A.L., 2013. Long-term outcomes of deep brain stimulation for neuropathic pain. Neurosurgery 72, 221–230. https://doi.org/10.1227/NEU.0b013e31827b97d6/.

Borsook, D., Sava, S., Becerra, L., 2010. The pain imaging revolution: advancing pain into the 21st century. Neuroscientist 16, 171–185. https://doi.org/10.1177/1073858409349902/.

Buzsaki, G., Draguhn, A., 2004. Neuronal oscillations in cortical networks. Science 304, 1926–1929. https://doi.org/10.1126/science.1099745/.

Carstens, E., Trevino, D.L., 1978. Laminar origins of spinothalamic projections in the cat as determined by the retrograde transport of horseradish peroxidase. J. Comp. Neurol. 182 (1), 151–165. https://doi.org/10.1002/(ISSN)1096-986110.1002/cne.v182:1.

Çavdar, S., Onat, F., Aker, R., Şehirli, U., Şan, T., Raci Yananli, H., 2001. The afferent connections of the posterior hypothalamic nucleus in the rat using horseradish peroxidase. J. Anat. 198 (4), 463–472. https://doi.org/10.1046/j.1469-7580.2001.19840463.x.

Davis, K.D., Flor, H., Greely, H.T., Iannetti, G.D., Mackey, S., Ploner, M., Pustilnik, A., Tracey, I., Treede, R.-D., Wager, T.D., 2017. Brain imaging tests for chronic pain: medical, legal and ethical issues and recommendations. Nat. Rev. Neurol. 13, 624–638. https://doi.org/10.1038/nrneurol.2017.122/.

Devinsky, O., Morrell, M.J., Vogt, B.A., 1995. Contributions of anterior cingulate cortex to behaviour. Brain 118, 279–306. https://doi.org/10.1093/brain/118.1.279/.

Donoho, D.L., Johnstone, I.M., 1994. Ideal spatial adaptation by wavelet shrinkage. Biometrika 81, 425–455. https://doi.org/10.1093/biomet/81.3.425.

Fields, H.L., 1999. Pain: an unpleasant topic. Pain 82, S61–S69. https://doi.org/10.1016/S0304-3959(99)00139-6/.

Gonzalez-Roldan, A.M., Cifre, I., Sitges, C., Montoya, P., 2016. Altered dynamic of EEG oscillations in fibromyalgia patients at rest. Pain Med. 17, 1058–1068. https://doi.org/10.1093/pm/pnw023/.

Gray, A.M., Pounds-Cornish, E., Eccles, F.J.R., Aziz, T.Z., Green, A.L., Scott, R.B., 2014. Deep brain stimulation as a treatment for neuropathic pain: a longitudinal study addressing neuropsychological outcomes. J. Pain 15, 283–292. https://doi.org/10.1016/j.jpain.2013.11.003/.

Green, A.L., Paterson, D.J., 2020. Using deep brain stimulation to unravel the mysteries of cardiorespiratory control. Compr. Physiol. 10, 1085–1104. https://doi.org/10.1002/cphy.c190039/.

Green, A.L., Wang, S., Stein, J.F., Pereira, E.A., Kringelbach, M.L., Liu, X., Brittain, J.S., Aziz, T.Z., 2009. Neural signatures in patients with neuropathic pain. Neurology 72, 569–571. https://doi.org/10.1212/01.wnl.0000342122.25498.8b/.

Hammond, C., Bergman, H., Brown, P., 2007. Pathological synchronization in Parkinson's disease: networks, models and treatments. Trends Neurosci. 30, 357–364. https://doi.org/10.1016/j.tins.2007.05.004/.

Hartley, C., Duff, E.P., Green, G., Mellado, G.S., Worley, A., Rogers, R., Slater, R., 2017. Nociceptive brain activity as a measure of analgesic efficacy in infants. Sci. Transl. Med. 9 https://doi.org/10.1126/scitranslmed.aah6122/.

Hauck, M., Lorenz, J., Engel, A.K., 2007. Attention to painful stimulation enhances gamma-band activity and synchronization in human sensorimotor cortex. J. Neurosci. 27, 9270–9277. https://doi.org/10.1523/jneurosci.2283-07.2007/.

Hu, L., Iannetti, G.D., 2019. Neural indicators of perceptual variability of pain across species. Proc. Natl. Acad. Sci. 116 (5), 201812499. https://doi.org/10.1073/pnas.1812499116/.

Huskisson, E.C., 1974. Measurement of pain. The Lancet 304(7889), 1127–1131. https://doi.org/10.1016/S0140-6736(74)90884-8.

Katz, Joel, Melzack, Ronald, 1999. Measurement of pain. Surg. Clin. N. Am. 79 (2), 231. https://doi.org/10.1016/s0039-6109(05)70381-9.

Keay, K.A., Feil, K., Gordon, B.D., Herbert, H., Bandler, R., 1997. Spinal afferents to functionally distinct periaqueductal gray columns in the rat: an anterograde and retrograde tracing study. J. Comp. Neurol. 385, 207–229. https://doi.org/10.1002/(SICI)1096-9861(19970825)385:2<207::AID-CNE3>3.0.CO;2-5/.

Krout, K.E., Loewy, A.D., 2000. Periaqueductal gray matter projections to midline and intralaminar thalamic nuclei of the rat. J. Comp. Neurol. 424, 111–141. https://doi.org/10.1002/1096-9861(20000814)424:1<111::aid-cne9>3.0.co;2-3/.

Li, J.-N., Sheets, P.L., 2018. The central amygdala to periaqueductal gray pathway comprises intrinsically distinct neurons differentially affected in a model of inflammatory pain. J. Physiol. 596 (24), 6289–6305. https://doi.org/10.1113/tjp.2018.596.issue-24.

Li, X., Zhao, Z., Ma, J., Cui, S., Yi, M., Guo, H., Wan, Y., 2017. Extracting neural oscillation signatures of laser-induced nociception in pain-related regions in rats. Front. Neural Circuits 11. https://doi.org/10.3389/fncir.2017.00071/.

Luo, H., Huang, Y., Du, X., Zhang, Y., Green, A.L., Aziz, T.Z., Wang, S., 2018. Dynamic neural state identification in deep brain local field potentials of neuropathic pain. Front. Neurosci. 12 https://doi.org/10.3389/fnins.2018.00237/.

Luo, H., Huang, Y., Xiao, X., Dai, W., Nie, Y., Geng, X., Green, A.L., Aziz, T.Z., Wang, S., 2019. Functional dynamics of thalamic local field potentials correlate with modulation of neuropathic pain. Eur. J. Neurosci. https://doi.org/10.1111/ejn.14569/.

Melzack, R., 1975. Mcgill pain questionnaire-major properties and scoring methods. Pain 1, 277–299. https://doi.org/10.1016/0304-3959(75)90044-5/.

Melzack, R., Stotler, W.A., Livingston, W.K., 1958. Effects of discrete brainstem lesions in cats on perception of noxious stimulation. J. Neurophysiol. 21, 353–367. https://doi.org/10.1097/00000542-200507000-00028/.

Michalareas, G., Vezoli, J., van Pelt, S., Schoffelen, J.M., Kennedy, H., Fries, P., 2016. Alpha-beta and gamma rhythms subserve feedback and feedforward influences among human visual cortical areas. Neuron 89, 384–397. https://doi.org/10.1053/eujp.2001.0259/.

Mouton, L.J., Holstege, G., 2000. Segmental and laminar organization of the spinal neurons projecting to the periaqueductal gray (PAG) in the cat suggests the existence of at least five separate clusters of spino-PAG neurons. J. Comp. Neurol. 428 (3), 389–410. https://doi.org/10.1016/s0304-3940(98)00723-x.

Nashold, B.S., Wilson, W.P., Slaughter, D.G., 1969. Sensations evoked by stimulation in midbrain of man. J. Neurosurg. 30, 14. https://doi.org/10.3171/jns.1969.30.1.0014/.

Neumann, W.J., Turner, R.S., Blankertz, B., Mitchell, T., Kuhn, A.A., Mark Richardson, R., 2019. Toward electrophysiology-based intelligent adaptive deep brain stimulation for movement disorders. Neurotherapeutics: J. Am. Soc. Exp. NeuroTherap. 2019. 10.1007/s13311-018-00705-0/.

Osaka, N., Osaka, M., Morishita, M., Kondo, H., Fukuyama, H., 2004. A word expressing affective pain activates the anterior cingulate cortex in the human brain: an fMRI study. Behav. Brain Res. 153, 123–127. https://doi.org/10.1016/j.bbr.2003.11.013/.

Parker, T., Huang, Y.Z., Raghu, A.L.B., FitzGerald, J.J., Green, A.L., Aziz, T.Z., 2020. Dorsal root ganglion stimulation modulates cortical gamma activity in the cognitive dimension of chronic pain. Brain Sci. 10 https://doi.org/10.3390/brainsci10020095/.

Pereira, E.A.C., Wang, S., Peachey, T., Lu, G., Shlugman, D., Stein, J.F., Aziz, T.Z., Green, A.L., 2013. Elevated gamma band power in humans receiving naloxone suggests dorsal periaqueductal and periventricular gray deep brain stimulation produced analgesia is opioid mediated. Exp. Neurol. 239, 248–255. https://doi.org/10.1016/j.expneurol.2012.10.017/.

Ploner, M., Sorg, C., Gross, J., 2017. Brain rhythms of pain. Trends Cogn. Sci. 21, 100–110. https://doi.org/10.1016/j.tics.2016.12.001/.

Price D, Donald, 2000. Neuroscience - Psychological and neural mechanisms of the affective dimension of pain. Science 288 (5472), 1769–1772. https://doi.org/10.1126/science.288.5472.1769.

Price D, Donald, 2002. Central neural mechanisms that interrelate sensory and affective dimensions of pain. Mol. Interven. 2, 392–403. https://doi.org/10.1124/mi.2.6.392.

Royce, G.J., Bromley, S., Gracco, C., 1991. Subcortical projections to the centromedian and parafascicular thalamic nuclei in the cat. J. Comp. Neurol. 306 (1), 129–155. https://doi.org/10.1002/(ISSN)1096-9861.

Russo, J.F., Sheth, S.A., 2015. Deep brain stimulation of the dorsal anterior cingulate cortex for the treatment of chronic neuropathic pain. Neurosurg. Focus 38. https://doi.org/10.3171/2015.3.focus1543/.

Sakurai, Y., 1999. How do cell assemblies encode information in the brain? Neurosci. Biobehav. Rev. 23, 785–796. https://doi.org/10.1016/s0149-7634(99)00017-2/.

Samineni, V.K., Premkumar, L.S., Faingold, C.L., 2017. Neuropathic pain induced enhancement of spontaneous and pain evoked neuronal activity in the periaqueductal gray that is attenuated by gabapentin. Pain 158 (7), 1241–1253. https://doi.org/10.1097/j.pain.0000000000000905.

Sarnthein, J., Jeanmonod, D., 2008. High thalamocortical theta coherence in patients with neurogenic pain. Neuroimage 39, 1910–1917. https://doi.org/10.1016/j.neuroimage.2007.10.019/.

Sarnthein, J., Morel, A., von Stein, A., Jeanmonod, D., 2003. Thalamic theta field potentials and EEG: high thalamocortical coherence in patients with neurogenic pain, epilepsy and movement disorders. Thalamus Relat. Syst. 2, 231–238. https://doi.org/10.1016/S1472-9288(03)00021-9/.

Shigenaga, Y., Nakatani, Z., Nishimori, T., Suemune, S., Kuroda, R., Matano, S., 1983. The cells of origin of cat trigeminothalamic projections: especially in the caudal medulla. Brain Res. 277 (2), 201–222. https://doi.org/10.1016/0006-8993(83)90928-9.

Shirvalkar, P., Veuthey, T.L., Dawes, H.E., Chang, E.F., 2018. Closed-loop deep brain stimulation for refractory chronic pain. Front. Comput. Neurosci. 12 https://doi.org/10.3389/fncom.2018.00018/.

Stern, J., Jeanmonod, D., Sarnthein, J., 2006. Persistent EEG overactivation in the cortical pain matrix of neurogenic pain patients. Neuroimage 31, 721–731. https://doi.org/10.1016/j.neuroimage.2005.12.042/.

Tinkhauser, G., Pogosyan, A., Little, S., Beudel, M., Herz, D.M., Tan, H., Brown, P., 2017a. The modulatory effect of adaptive deep brain stimulation on beta bursts in Parkinson's disease. Brain 140, 1053–1067. https://doi.org/10.1093/brain/awx010/.

Tinkhauser, G., Pogosyan, A., Tan, H.L., Herz, D.M., Kuhn, A.A., Brown, P., 2017b. Beta burst dynamics in Parkinson's disease OFF and ON dopaminergic medication. Brain 140, 2968–2981. https://doi.org/10.1093/brain/awx252/.

Todd, K.H., 1996. Clinical versus statistical significance in the assessment of pain relief. Ann. Emerg. Med. 27 (4), 439–441. https://doi.org/10.1016/S0196-0644(96)70226-3.

Tracey, I., Ploghaus, A., Gati, J.S., Clare, S., Smith, S., Menon, R.S., Matthews, P.M., 2002. Imaging attentional modulation of pain in the periaqueductal gray in humans. J. Neurosci. 22(7), 2748–2752. https://doi.org/20026238.

Wager, T.D., Atlas, L.Y., Lindquist, M.A., Roy, M., Woo, C.W., Kross, E., 2013. An fMRI-based neurologic signature of physical pain. N. Engl. J. Med. 368, 1388–1397. https://doi.org/10.1056/NEJMoa1204471/.

Wang, J., Wang, J., Xing, G.G., Li, X.L., Wan, Y., 2016. Enhanced gamma oscillatory activity in rats with chronic inflammatory pain. Front. Neurosci. 10 https://doi.org/10.3389/fnins.2016.00489/.

Wu, D., Wang, S., Stein, J.F., Aziz, T.Z., Green, A.L., 2014. Reciprocal interactions between the human thalamus and periaqueductal gray may be important for pain perception. Exp. Brain Res. 232, 527–534. https://doi.org/10.1007/s00221-013-3761-4/.

Vanderhorst, V.G., Mouton, L.J., Blok, B.F., Holstege, G., 1996. Distinct cell groups in the lumbosacral cord of the cat project to different areas in the periaqueductal gray. J. Comp. Neurol. 376 (3), 361–385. https://doi.org/10.1002/(SICI)1096-9861(19961216)376:3<361::AID-CNE2>3.0.CO;2-0.

Xiao, X., Zhang, Y.Q., 2018. A new perspective on the anterior cingulate cortex and affective pain. Neurosci. Biobehav. Rev. 90, 200–211. https://doi.org/10.1016/j.neubiorev.2018.03.022/.

Xu, M., Fei, Y., He, Q., Fu, J., Zhu, J., Tao, J., Ni, C., Xu, C., Zhou, Q., Yao, M., Ni, H., 2021. Electroacupuncture attenuates cancer-induced bone pain via NF-κB/CXCL12 signaling in midbrain periaqueductal gray. ACS Chem. Neurosci. 12 (18), 3323–3334. https://doi.org/10.1021/acschemneuro.1c00224.

Yue, L., Iannetti, G.D., Hu, L., 2020. The neural origin of nociceptive-induced gamma-band oscillations. J. Neurosci. 40, 3478–3490. https://doi.org/10.1523/jneurosci.0255-20.2020/.

Yu, W., Pati, D., Pita, D., Pina, M.M., Schmidt, K.T., Boyt, K.M., Hunker, A.C., Zweifel, L. S., McElligott, Z.A., Kash, T.L., 2021. Periaqueductal gray/dorsal raphe dopamine neurons contribute to sex differences in pain-related behaviors. Neuron 109 (8), 1365–1380. https://doi.org/10.1016/j.neuron.2021.03.001.

Zhang, S., Green, A., Smith, P.P., 2013. An automatic classifier of pain scores in chronic pain patients from local field potentials recordings. In: 2013 6th International IEEE/EMBS Conference on Neural Engineering, pp. 1194–1197. https://doi.org/10.1109/NER.2013.6696153/.

Zhou, R., Wang, J., Qi, W.J., Liu, F.Y., Yi, M., Guo, H.L., Wan, Y., 2018. Elevated resting state gamma oscillatory activities in electroencephalogram of patients with post-herpetic neuralgia. Front. Neurosci. 12, 10. https://doi.org/10.3389/fnins.2018.00750/.